Spin and Orbital Magnetic Moments of Fe_3O_4

D. J. Huang,[1,2] C. F. Chang,[1] H.-T. Jeng,[3] G. Y. Guo,[4,1] H.-J. Lin,[1] W. B. Wu,[2,1] H. C. Ku,[5] A. Fujimori,[6] Y. Takahashi,[7] and C. T. Chen[1]

[1]*National Synchrotron Radiation Research Center, Hsinchu 30077, Taiwan*
[2]*Department of Electrophysics, National Chiao-Tung University, Hsinchu 300, Taiwan*
[3]*Physics Division, National Center for Theoretical Sciences, Hinchu 300, Taiwan*
[4]*Department of Physics, National Taiwan University, Taipei 106, Taiwan*
[5]*Department of Physics, National Tsing Hua University, Hsinchu 300, Taiwan*
[6]*Department of Complexity Science and Engineering and Department of Physics, University of Tokyo, Tokyo 113-0033, Japan*
[7]*Graduate School and Faculty of Science, Himeji Institute of Technology, Hyogo 678-1297, Japan*

(Received 9 January 2004; published 11 August 2004)

We present measurements of the spin and orbital magnetic moments of Fe_3O_4 by using SQUID and magnetic circular dichroism in soft x-ray absorption. The measurements show that Fe_3O_4 has a noninteger spin moment, in contrast to its predicted half-metallic feature. Fe_3O_4 also exhibits a large unquenched orbital moment. Calculations using the local density approximation including the Hubbard U method and the configuration interaction cluster-model suggest that strong correlations and spin-orbit interaction of the $3d$ electrons result in the noninteger spin and large orbital moments of Fe_3O_4.

DOI: 10.1103/PhysRevLett.93.077204 PACS numbers: 75.50.Ss, 71.28.+d, 75.25.+z, 78.70.Dm

Magnetite (Fe_3O_4) exhibits many interesting properties such as charge ordering, mixed valence, and metal-insulator transition known as the Verwey transition [1], in which the conductivity decreases by 2 orders of magnitude upon cooling through the transition temperature $T_V \sim 120$ K. In spite of intensive studies on its electronic structure, surprisingly, no consensus has been reached concerning the electronic nature of Fe_3O_4. Experimental studies, including neutron diffuse scattering [2], NMR [3], and x-ray scattering [4,5], indicate that Fe_3O_4 should be considered as an itinerant magnet rather than a fluctuating mixed-valence material. According to band theory, Fe_3O_4 is a half-metal above T_V; its minority-spin electrons are conducting, whereas the majority-spin ones are insulating [6]. In addition, Fe_3O_4 would have an integral spin moment per formula unit (f.u.), i.e., $4.0\mu_B$; the orbital moment of metallic Fe_3O_4 would be quenched.

On the other hand, charge ordering of the octahedral (B-site) Fe in Fe_3O_4 has been suggested by the refinements of x-ray and neutron diffraction data [7], implying that the $3d$ electrons of Fe_3O_4 have a strong localized character. Fe^{2+} in Fe_3O_4 is thus expected to exhibit a large unquenched orbital moment, like Fe^{2+} in FeO [8]. Theoretical and experimental works show that localization of the $3d$ electrons of transition-metal compounds leads to giant orbital moments. For example, FeO [8], CoO [9], Fe impurities in alkali metals [10], and Fe nitridometalates [11] are shown to have giant or unquenched orbital moments. In addition, calculations based on atomic multiplet theory show that the localized nature of the open $3d$ shell of Fe_3O_4 sets a limit of -66.7% on the spin polarization of conduction electrons [12], rather than -100% predicted by band theory. Results of spin-resolved photoemission from epitaxial thin films and single crystals of Fe_3O_4 support the conclusion of multiplet calculations [13–16], in contrast to the conclusion from spin-resolved photoemission of $Fe_3O_4(111)$ thin films grown on W(110) [17].

Measurements of orbital and spin moments therefore provide an opportunity to explore the character of $3d$ electrons in Fe_3O_4 [18,19]. Examining whether Fe_3O_4 has a quenched orbital moment and an integral spin moment is important in revealing its electronic nature.

In this Letter, we present studies of the spin and orbital moments of Fe_3O_4 single crystals by combining magnetic circular dichroism (MCD) in soft x-ray absorption spectroscopy (XAS) and measurements using a superconducting quantum interference device (SQUID) magnetometer. In addition, we performed cluster-model calculations in the configuration interaction (CI) approach and band-structure calculations in the local spin density approximation including the on-site Coulomb interaction U (LDA + U) [20,21] to unravel the underlying physics of the magnetic moments of Fe_3O_4.

Single crystals of Fe_3O_4 were grown by the floating zone method and fully characterized by x-ray diffraction. Temperature-dependent measurements of the resistance of the crystal show an abrupt change at 120 K, as plotted in Fig. 3(a), revealing the Verwey transition of Fe_3O_4. We measured the total magnetic moment of a 21.59-mg Fe_3O_4 single crystal with an applied field of 1 T along the [111] direction using a SQUID magnetometer.

We measured MCD in XAS on Fe_3O_4 at various temperatures under an applied magnetic field of 1 T along the [111] direction using the Dragon beam line at the National Synchrotron Radiation Research Center in Taiwan. XAS spectra of Fe_3O_4 were taken in the total electron yield (TEY) mode with a photon-energy resolution of 0.2 eV

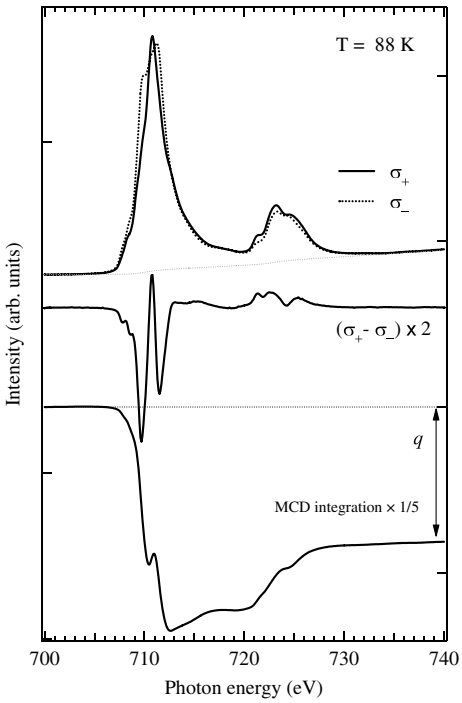

FIG. 1. Fe $L_{2,3}$-edge XAS and MCD spectra of Fe_3O_4 with correction for the saturation effect. Top: XAS spectra with spin of photons parallel and antiparallel to that of Fe $3d$ majority electrons. The XAS background is depicted in a thin dotted line. Middle: MCD spectrum, i.e., $(\sigma_+ - \sigma_-) \times 2$. Bottom: integration of MCD. Spectra of MCD and MCD integration are plotted with different vertical offsets for clarity.

and an incident angle of 60°. The degree of circular polarization of the incident light was 80%. The crystal was freshly cleaved in an ultrahigh vacuum at 90 K; the fracture plane of the sample is normal to the [110] direction. We take our MCD measurements to be representative of bulk Fe_3O_4, because the probing depth of the TEY method is around 50 Å or deeper.

The sum rules of MCD in x-ray absorption permit an element-selective separation of the spin and orbital contributions to the total magnetic moment of materials [22–26]. The total orbital moment m_{orb} per formula of Fe_3O_4 can be expressed as [27]

$$m_{\mathrm{orb}} = -\frac{4}{3}\frac{\int_{L_{2,3}}(\sigma_+ - \sigma_-)d\omega}{\int_{L_{2,3}}(\sigma_+ + \sigma_-)d\omega}N^h, \qquad (1)$$

in which σ_+ and σ_- are the absorption cross sections taken with the projection of spin of incident photons parallel and antiparallel to those of the majority of $3d$ electrons, respectively. In addition, ω is the photon energy; N^h is the total number of Fe $3d$ holes per formula unit.

XAS recorded with the TEY method suffers typically from the saturation effects, leading to an inaccurate measure of orbital moments [28]. The measured absorption I_{TEY} in a TEY measurement is reduced by a factor of $f = 1/(1 + \lambda_e/\lambda_x \cos\theta)$, where λ_x and λ_e are the photon penetration depth and the electron sampling depth, respectively, and θ is the incidence angle of x ray with respect to the surface normal [28]. λ_e was estimated to be 50 Å for Fe_3O_4 [29]. By using quasitransmission measurements of XAS, we have determined the photon-energy-dependent λ_x of Fe_3O_4 to correct our XAS and MCD measurements for the saturation effects [30]. λ_x at the L_3 and L_2 edges are, respectively, 254 and 653 Å.

Figure 1 displays Fe $L_{2,3}$-edge XAS and MCD spectra of Fe_3O_4 single crystals measured at 88 K using the TEY method. Our XAS and MCD spectra are similar to those of epitaxial Fe_3O_4 thin films [31,32]. The XAS background shown in Fig. 1 is composed of an arctangentlike edge-jump function and a linear function. With $N^h = 13.5$ [33] and taking the geometric effect in absorption and the degree of circular polarization of incident photons into account, we obtained m_{orb} of Fe_3O_4 at various temperatures, as summarized in Table I. The uncertainty in determining m_{orb} originates mainly from the background function of XAS. Our measurements unravel that Fe_3O_4 exhibits an unquenched orbital moment. For example, the measured orbital moment m_{orb} is 0.65 ± 0.07 at $T = 145$ K. In other words, the average orbital moment per B-site Fe is $0.33 \pm 0.04\mu_B$, because the orbital moment of A-site Fe^{3+} is insignificant according to Hund's rule and the local density approximation (LDA) and the local density approximation with Hubbard U (LDA + U) calculations described later; such an unquenched orbital moment is much larger than that of Fe metal, $0.09\mu_B$ [25].

To comprehend the underlying physics of an unquenched orbital moment of Fe_3O_4, we performed band-structure calculations on its cubic phase using the all-electron full potential linear muffin-tin orbital method including the spin-orbit interaction [35] within the LDA and LDA + U schemes. Both LDA [6] and LDA + U calculations [36] conclude that cubic Fe_3O_4 is half-metallic and has a spin moment of $4.0\mu_B$ per f.u. as summarized in Table II. Also the orbital moment of A-site Fe ions is insignificant ($\sim -0.02\mu_B$), as expected from Hund's coupling of a half-filled Fe^{3+}. LDA calculations give rise to a nearly quenched orbital moment of Fe_3O_4. On the other hand, an unquenched orbital moment of $0.21\mu_B$ per B-site Fe atom was obtained by the LDA + U calculations [37], indicating that the Coulomb interactions of $3d$ electrons lead to the unquenched orbital moment. To demonstrate such an effect, we calculated the occupation numbers and charge densities of the B-site $3d$

TABLE I. Measured m_{orb} of Fe_3O_4 from MCD at various temperatures.

T (K)	88	100	145	200
m_{orb}	0.76 ± 0.09	0.66 ± 0.07	0.65 ± 0.07	0.67 ± 0.08

TABLE II. Calculated and measured (at $T = 145$ K) magnetic moments of Fe_3O_4. Total spin (m_{spin}) and orbital (m_{orb}) moments per f.u. of Fe_3O_4, and average orbital moment (m^B_{orb}) per B-site Fe atom are displayed in units of μ_B.

	m_{spin}	m_{orb}	m^B_{orb}	m_{orb}/m_{spin}
LDA	4.0	0.06	0.04	0.015
LDA + U	4.0	0.43	0.21	0.108
Expt.	3.68 ± 0.09	0.65 ± 0.07	0.33 ± 0.04	0.18

down-spin states projected to orbitals with different magnetic quantum numbers m. Without inclusion of the Coulomb interaction U, the projected occupation number of B-site $3d$ electrons distributes almost evenly onto orbitals of different magnetic quantum numbers; the orbital moment is thus quenched. With inclusion of U, on the other hand, the occupation number of the $m = 1$ state is drastically enhanced, and that of the $m = -1$ state is suppressed, resulting in a strong orbital polarization and a large orbital moment of B-site Fe, as presented in Fig. 2.

We also calculated the magnetic moments of octahedral Fe using a configuration interaction (CI) cluster model including spin-orbit interaction [32,39]. The results suggest that the octahedral Fe^{2+} in a FeO_6^{10-} cluster exhibits a spin moment of $3.74\mu_B$ and an orbital moment of $0.97\mu_B$, implying an average orbital moment of $0.48\mu_B$ per B-site Fe atom in Fe_3O_4 [32]. The measured average orbital moment of $0.33 \pm 0.04\mu_B$ per B-site Fe thus indicates that the $3d$ electrons of Fe_3O_4 have a strongly correlated electronic nature even at temperatures above T_V.

To quantitatively determine the total spin moment m_{spin} per formula unit of Fe_3O_4, we measured also the total magnetic moment of Fe_3O_4 at the temperatures between 80 and 200 K by using a SQUID magnetometer, as plotted in Fig. 3(b). Combining the MCD and SQUID measurements, we then obtained m_{spin} at various temperatures, because both LDA and LDA + U calculations conclude that the orbital moment of oxygen is negligible. Our measurements indicate that the spin and orbital moments of Fe_3O_4 do not change significantly around the temperature T_V. In addition, Fe_3O_4 exhibits a noninteger spin moment. For example, the total magnetic moment of Fe_3O_4 at $T = 145$ K is $4.33\mu_B$; with the measured m_{orb} of 0.65 ± 0.07, remarkably m_{spin} per f.u. of Fe_3O_4 is $3.68 \pm 0.09\mu_B$, as displayed in Table II, in contrast to the integral spin moment of $4.0\mu_B$ as a result of half-metallic behavior predicted by band theory. With CI calculations, we found that the spin moment of octahedral Fe^{2+} in a FeO_6^{10-} cluster is suppressed by ~5% if the strength of the spin-orbit interaction of $3d$ electrons is doubled, whereas the integral spin moment of Fe_3O_4 obtained from LDA + U calculations is rather insensitive to the strength of spin-orbit coupling. This observation suggests that the observed noninteger spin moment is beyond the Bloch electron picture and might result from a combined effect of the spin-orbit interaction and strong correlations of the $3d$ electrons in Fe_3O_4.

With measurements of SQUID and MCD in soft x-ray absorption, we can also study the spin moment of oxygens in Fe_3O_4. The spin sum rule of MCD [23] correlates the total spin moment m^{Fe}_{spin} of Fe in Fe_3O_4 to the MCD data as $m^{Fe}_{spin} + 7\langle T_z\rangle = -\frac{6p-4q}{I}N^h$, in which p and q are defined as MCD integrations $\int_{L_3}(\sigma_+ - \sigma_-)d\omega$ and $\int_{L_3+L_2}(\sigma_+ - \sigma_-)d\omega$, respectively, and I as the XAS integration. In addition, $\langle T_z\rangle$ is the expectation value of magnetic dipole

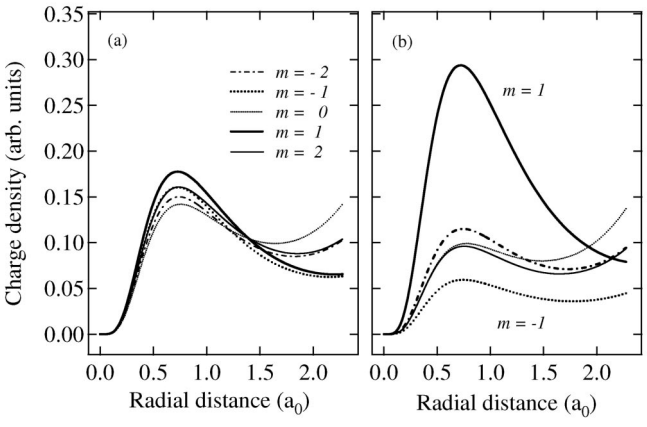

FIG. 2. Charge densities of cubic Fe_3O_4 versus radial distance in units of atomic radius a_0. The charge densities projected to different orbitals with magnetic quantum number m were obtained from (a) LDA and (b) LDA + U calculations.

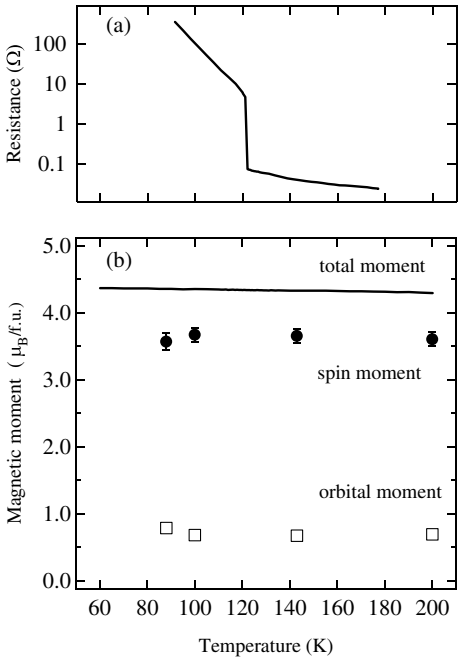

FIG. 3. (a) Resistance of a Fe_3O_4 single crystal in the vicinity of the Verwey transition. (b) Total magnetic moment, spin, and orbital moments of Fe_3O_4 at various temperatures.

operator. By using the spin sum rule with correction for its deviation resulting from the intermixing between the L_2 and L_3 edges [40], we obtained a value of $3.55\mu_B$ for $m_{\text{spin}}^{\text{Fe}} + 7\langle T_z\rangle$ at $T = 145$ K. Our LDA + U calculations disclose that $7\langle T_z\rangle$ per B-site Fe atom is $0.155\mu_B$, whereas $7\langle T_z\rangle$ of the A-site Fe atoms is $-0.0001\mu_B$. The significant $7\langle T_z\rangle$ value of the B-site Fe atoms is caused by their strong orbital polarization as shown in Fig. 2. The total spin moment $m_{\text{spin}}^{\text{Fe}}$ of Fe in Fe_3O_4 is therefore $3.24\mu_B$, leading to a spin moment of $0.44\mu_B$ originating from oxygen atoms per Fe_3O_4, i.e., a spin moment of $0.11\mu_B$ per O atom in Fe_3O_4. This deduced spin moment of oxygen is close to the calculated spin moment of $0.07\mu_B$ per O atom from our LDA + U calculations and consistent with LDA calculations [6,42].

In conclusion, we have measured the orbital and spin magnetic moments of Fe_3O_4 by combining SQUID and MCD. We found that Fe_3O_4 has a noninteger spin moment, in contrast to its predicted half-metallic feature, and that the average orbital moment of B-site Fe in Fe_3O_4 is significantly larger than that of Fe metal. As evidenced by LDA + U calculations, the on-site Coulomb interactions of $3d$ electrons result in the unquenched orbital moment and magnetic dipole moment of Fe_3O_4. Our results suggest that spin-orbit interaction and electron correlations of $3d$ electrons play an important role in the spin and orbital moments of Fe_3O_4. We call for further theoretical work on the magnetic moments of Fe_3O_4.

We acknowledge S. Kimura for providing Fe_3O_4 single crystals, A. Tanaka for sharing the computation code of the CI calculation, and C.-M. Huang and C.-H. Hsu for characterizing the orientation of the fracture plane of the Fe_3O_4 sample. We thank L. H. Tjeng, T. Jo, C. H. Chen, and C. S. Hsue for valuable discussions. This work was supported in part by the National Science Council of Taiwan and by a Grant-in-Aid for Scientific Research in Priority Area "Novel Quantum Phenomena in Transition-Metal Oxides" from the Ministry of Education, Culture, Sports, Science and Technology of Japan.

[1] E. J. W. Verwey, Nature (London) **144**, 327 (1939).
[2] K. Siratori *et al.*, J. Phys. Soc. Jpn. **67**, 2818 (1998).
[3] P. Novak *et al.*, Phys. Rev. B **61**, 1256 (2000).
[4] J. Garcia *et al.*, Phys. Rev. B **63**, 054110 (2001).
[5] J. Garcia *et al.*, Phys. Rev. Lett. **85**, 578 (2000).
[6] For example, see H.-T. Jeng and G. Y. Guo, Phys. Rev. B **65**, 094429 (2002).
[7] J. P. Wright, J. P. Attfield, and P. G. Radaelli, Phys. Rev. Lett. **87**, 266401 (2001).
[8] A. Svane and O. Gunnarsson, Phys. Rev. Lett. **65**, 1148 (1990); T. Jo and T. Shishidou, J. Phys. Soc. Jpn. **67**, 2505 (1998).
[9] W. Neubeck *et al.*, J. Phys. Chem. Solids **62**, 2173 (2001).
[10] S. K. Kwon and B. I. Min, Phys. Rev. Lett. **84**, 3970 (2000); G. Y. Guo, Phys. Rev. B **62**, R14 609 (2000); P. Gambardella *et al.*, Phys. Rev. Lett. **88**, 047202 (2002).
[11] J. Klatyk *et al.*, Phys. Rev. Lett. **88**, 207202 (2002).
[12] S. F. Alvarado *et al.*, Phys. Rev. Lett. **35**, 860 (1975); S. F. Alvarado and P. S. Bagus, Phys. Lett. **67A**, 397 (1978).
[13] S. F. Alvarado *et al.*, Phys. Rev. Lett. **34**, 319 (1975).
[14] S. F. Alvarado, M. Erbudak, and P. Munz, Phys. Rev. B **14**, 2740 (1976).
[15] H.-J. Kim, J.-H. Park, and E. Vescovo, Phys. Rev. B **61**, 15 288 (2000).
[16] D. J. Huang *et al.*, J. Magn. Magn. Mater. **239**, 261 (2002).
[17] Yu. S. Dedkov, U. Rudiger, and G. Guntherodt, Phys. Rev. B **65**, 064417 (2002).
[18] I. V. Solovyev, A. I. Liechtenstein, and K. Terakura, Phys. Rev. Lett. **80**, 5758 (1998).
[19] S. K. Kwon and B. I. Min, Phys. Rev. B **62**, 73 (2000).
[20] V. I. Anisimov, J. Zaanen, and O. K. Andersen, Phys. Rev. B **44**, 943 (1991).
[21] A. I. Liechtenstein, V. I. Anisimov, and J. Zaanen, Phys. Rev. B **52**, R5467 (1995).
[22] B. T. Thole *et al.*, Phys. Rev. Lett. **68**, 1943 (1992).
[23] P. Carra *et al.*, Phys. Rev. Lett. **70**, 694 (1993).
[24] R. Wu and A. J. Freeman, Phys. Rev. Lett. **73**, 1994 (1994).
[25] C. T. Chen *et al.*, Phys. Rev. Lett. **75**, 152 (1995).
[26] G. Y. Guo, Phys. Rev. B **57**, 10 295 (1998).
[27] $m_{\text{orb}} = -\frac{4}{3}\left(\frac{q_A N_A^h}{I_A} + \frac{q_{B_2} N_{B_2}^h}{I_{B_2}} + \frac{q_{B_3} N_{B_3}^h}{I_{B_3}}\right)$, in which q and I are MCD and XAS integrations; subscripts A, B_2, and B_3 denote A-site Fe^{3+}, B-site Fe^{2+}, and Fe^{3+}, respectively. Note that $\frac{N_A^h}{I_A} = \frac{N_{B_2}^h}{I_{B_2}} = \frac{N_{B_3}^h}{I_{B_3}}$.
[28] R. Nakajima, J. Stohr, and Y. U. Idzerda, Phys. Rev. B **59**, 6421 (1999).
[29] S. Gota *et al.*, Phys. Rev. B **62**, 4187 (2000).
[30] D. J. Huang *et al.*, J. Electron Spectrosc. Relat. Phenom. **137C–140C**, 633 (2004).
[31] P. Kuiper *et al.*, J. Electron Spectrosc. Relat. Phenom. **86**, 107 (1997).
[32] J. Chen *et al.*., Phys. Rev. B **69**, 085107 (2004).
[33] According to the measurements of Fe $2p$ core-level photoemission [34], the net numbers of $3d$ electrons of Fe^{3+} and Fe^{2+} are, respectively, 5.3 and 6.1, suggesting 16.7 electrons in the $3d$ bands per formula unit of Fe_3O_4. In addition, the LDA + U calculations show that the number of $3d$ electrons of Fe_3O_4 is 16.32. Thus $N^h \sim 13.5 \pm 0.2$.
[34] T. Saitoh *et al.*, Phys. Rev. B **52**, 7934 (1995).
[35] S. Y. Savrasov, Phys. Rev. B **54**, 16 470 (1996).
[36] LDA + U calculations were carried out with $J = 0.89$ eV, $U = 4.5$ eV for A-site Fe, and $U = 4.0$ eV for B-site Fe.
[37] We used the rotationally invariant LDA + U functional [21]. With the original LDA + U functional [20], we obtained insignificant orbital moments (within $0.04\mu_B$/atom), being consistent with a recent report [38].
[38] V. N. Antonov *et al.*, Phys. Rev. B **64**, 134410 (2001).
[39] A. Tanaka and T. Jo, J. Phys. Soc. Jpn. **63**, 2788 (1994).
[40] Teramura *et al.* found that the spin sum rule underestimates the spin moment of a $3d^6$ system by 10% [41].
[41] Y. Teramura, A. Tanaka, and T. Jo, J. Phys. Soc. Jpn. **65**, 1053 (1996).
[42] Z. Zhang and S. Satpathy, Phys. Rev. B **44**, 13 319 (1991).